Fusion Using Fast Heating of a Compactly Imploded CD Core

Y. Kitagawa, Y. Mori, O. Komeda, K. Ishii, R. Hanayama, K. Fujita, S. Okihara, T. Sekine, N. Satoh, T. Kurita, M. Takagi, T. Kawashima, H. Kan, N. Nakamura, T. Kondo, M. Fujine, H. Azuma, T. Motohiro, T. Hioki, Y. Nishimura, A. Sunahara, and Y. Sentoku

Phys. Rev. Lett. **108**, 155001 — Published 9 April 2012

DOI: 10.1103/PhysRevLett.108.155001

Fusions using Fast Heating of a Compactly Imploded CD Core

Y. Kitagawa,* Y. Mori, O. Komeda, K. Ishii, R. Hanayama, K. Fujita, and S. Okihara
The Graduate School for the Creation of New Photonics Industries, Kurematsuchou, 1955-1 Nishi-ku, Hamamatsu 431-1202 Japan

T. Sekine, N. Satoh, T. Kurita, M. Takagi, T. Kawashima, and H. Kan
Hamamatsu Photonics, K. K. Kurematsuchou,1820 Nishi-ku, Hamamatsu 431-1202 Japan

N. Nakamura, T. Kondo, and M. Fujine
Advanced Material Engineering Div., TOYOTA Motor Corporation, 1200, Mishuku, Susono, Shizuoka, 410-1193 Japan

H. Azuma, T. Motohiro, and T. Hioki
TOYOTA Central Research and Development Laboratories, Inc., 41-1Yokomichi, Nagakute-cho, Aichi, Japan

Y. Nishimura
Toyota Technical Development Corp., 1-21 Imae, Hanamoto-cho, Toyota, Aichi, 470-0334 Japan

A. Sunahara
Institute for Laser Technology, 1-8-4 Utsubo-honmachi, Nishi-ku, Osaka, 550-0004 Japan

Y. Sentoku
Department of Physics, University of Nevada, Reno 1664 N VIRGINIA ST Reno, NV 89557

(Dated: February 21, 2012)

A compact fast core heating experiment is described. A 4J/0.4-ns output of an LD-pumped high-repetition laser HAMA is divided into four beams, two of which counter illuminate double deuterated polystyrene foils separated by 100 μm for implosion. The remaining two beams, compressed to 110 fs for fast heating, illuminate the same paths. Hot electrons produced by the heating pulses heat the imploded core, emitting X-ray radiations >40 eV and yielding some 10^3 thermal neutrons.

PACS numbers: 52.57.-z, 52.57.Fg, 79.20.Eb, 42.55.X, 28.52.Cx

The concept behind the fast ignitor scheme in inertial confinement fusion involves the preimplosion of a deuterium-tritium capsule to an isochoric condition[1]. At the maximum compression timing, the imploded core is irradiated with a laser pulse in a few tens of a picosecond, which is much shorter than the hydrodynamic disassembly time of the irradiated spot. Such a short-pulse laser generates hot electrons at the cutoff region, which penetrate into the core and form a hot spot. From the spot, the α burning wave spreads over the core.

In 2001 and 2002, a cone-guided PW laser[2] enhanced the neutron yield by two orders of magnitude from the imploded plasmas[3, 4]. In 2005, the PW laser was used again, but without a cone guide, to directly heat the imploded core and enhance neutrons[5].

However, the hot electrons deposit a fraction of their energy between the cutoff point and the ablation surface, before reaching the core. The implementation of the fast core heating might require the PW laser channeling close to the dense core plasma[6]. The problem of electron generation, transport and deposition has been extensively studied [for instance [7–10]] with growing evidence that the electrons can carry energy into the core.

Here, using a simple implosion scheme, we show that the hot electrons deposit energy to the peripheral plasma before reaching the ablation surface and also they reach the core and deposit some energy in it to emit x-ray radiations. Based on the neutron yields observed in the experiment the core is supposedly heated up to a few hundred electronvolts of temperature as long as the core stagnates. We discuss the heating process by one-dimensional integrated simulation of hydrodynamic and particle-in-cell (PIC) simulations.

We used an LD-pumped high-repetition-rate HAMA laser[11, 12], which consists of a seed beam supplier laser "BEAT", a Ti:sapphire optical parametric chirped pulse amplification system (OPCPA) [13], and a pump laser "KURE-I", an LD-pumped Nd:glass laser system (Hamamatsu Photonics)[14]. The latter pumps a Ti:sapphire crystal (50-mm diameter and 20-mm length) to amplify the seed beam from "BEAT".

The amplified chirped pulse of 3.6 J-800 nm in the 0.4-ns pulse is divided into two beams, one for imploding and another for heating the imploded core. The imploding beam is divided into two beams (Long beam-1 and Long beam-2), which are transported using different paths to

the target chamber. The remaining beam is time-delayed and pulse-compressed to a 110-fs Gaussian beam by two pairs of gold-coated plane gratings (1740 grooves/mm). This beam is then divided into two heating beams (Short beam-1 and Short beam-2). Short beam-1 is co-aligned to Long beam-1 and Short beam-2 to Long beam-2, respectively. A cross-beam divider stage enables us to coalign the four beams to counter-illuminate both sides of a target. The beam diameter is 60 mm.

A pair of off-axial 7.6-cm-diameter dielectric-coated mirror (OAP) counter-focused the beams, such that Long beam-1 and Short beam-1 are focused from the right-hand direction of the target and Long beam-2 and Short beam-2 approach from the left-hand side as shown in FIG.1(a). The focal length is 165 mm. All the beams are p-polarized on the target. The focal spot size w_0 is 32 μm (the energy concentration in the spot is 17%) and the pointing accuracy on the target is within ± 50 μm, or ± 0.3 mrad.

As shown in FIG.1(b), the target consists of two parallel 2-mm square plain foils. The foil is made of deuterated polystyrene ($(C_8D_8)_n$ or simply CD) and is 11 μm thick, supported with 100-μm-thick stainless steel. The separation (gap) between the foils is 100 μm. The target surface is tilted 1.3° from the laser axis to protect the laser optics from the back reflections. We set the focal position of the beams at the center between the double foils. Although the focal position of the short beam must be at the cutoff point of the ablated plasma, which is a few tens of μm far from the core, we have so far observed no clear difference by changing the position. This is because the focal spot size w_0 is 32 μm and the resulting Rayleigh length z_R is $\pi w_0^2/4\lambda = 1$mm.

The setup permits us to fire 100 shots continuously in a few minutes. Table I lists the on-target intensities of the beams. The OPCPA preamplifier perfectly suppresses prepulses, but the amplified spontaneous emissions (ASE) remain. To date, the second-harmonic probe light has observed no apparent preplasmas.

TABLE I. Energy and target intensity for the four beams

	$\ll$ *Imploding*	*beam* $\gg$	$\ll$ *Heating*	*beam* $\gg$
Beam#	**Long-1**	**Long-2**	**Short-1**	**Short-2**
Pulse width	404 ± 25 ps	404 ± 25 ps	110 ± 13 fs	110 ± 13 fs
Energy [J]	0.57 ± 0.02	0.53 ± 0.01	0.50 ± 0.01	0.46 ± 0.01
Intensity	5.9 ± 0.5	5.5 ± 0.5	1.9 ± 0.3	1.7 ± 0.3
[W/cm^2]	$\times 10^{13}$	$\times 10^{13}$	$\times 10^{17}$	$\times 10^{17}$

In FIG.1(c), a one-dimensional hydrodynamic code STAR[15] predicted that for 11-μm-thick foils with 100-μm gap, the target rear surfaces meet each other around 1.4 ns after the imploding beam peak, where the maximum compression occurs. We varied the heating pulse delay up to 2.0 ns.

A part of the pulse-compressed beam is converted to the second harmonics (400-nm wavelength) to probe the plasma collision. The probe captures shots of the double foil shadows, before the shot in FIG.2(a), and just when the compressed core is formed, as in FIG.2(b). The probe cutoff density n_c is 6×10^{21}cm^{-3}. The collecting lens NA = 7.18 is to take the core image up to $0.1n_c$. FIGURE 2(b) occurs 1.3 ns after the compression beam peak and marks the instance of the heating beam illumination. At this time the imploding beams are no longer present. The probe axis is perpendicular to the main beam axis. The plasma image is relayed through an interference filter (394±15 nm) to an ICCD camera that is open for 20 ns. In the phenomenon depicted in FIGs. 2(a) and (b), the foil thickness is 11 μm and the gap separation is 100 μm. Since the target is tilted at 1.3°, the foil shadow is observed to be 45 μm thick, not 11 μm thick. At this time, the formed core expands radially. On the outer boundary, the shallow dents, shown by arrows, appear correlated to the heating beams.

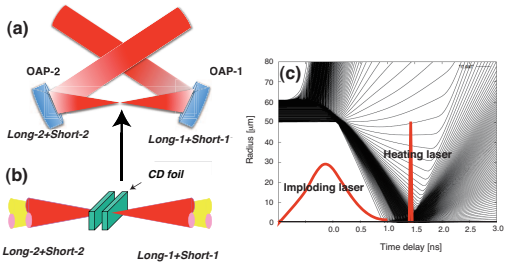

FIG. 1. (a) Counter-illumination scheme and (b) Double foil CD target. Imploding Long beam-1,-2 (red) are followed by heating Short beam-1,-2 (yellow). Long and Short beams are coaligned on both sides. (c)STAR 1D hydrodynamic flowchart (R-T diagram). Laser: 5×10^{13} W/cm^2. CD thickness is 11 μm and gap separation is 100 μm. The imploding (400 ps) and the heating beam (110 fs) positions are plotted on the chart.

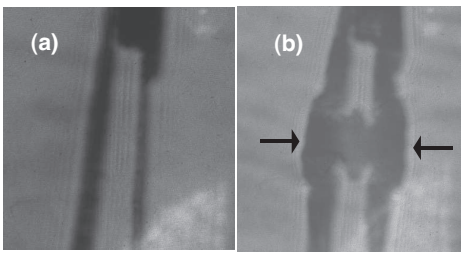

FIG. 2. (a) 2ω 100-fs probe captures the double foil image before the shot and (b) the moment occuring 1.3 ns after the peak of the imploding beam, when the imploded plasmas collide with each other and form the core. A stainless steel supports(upper in the figure) the double foils. The probe is synchronized with the heating beam. The probe axis is perpendicular to the main beam axis. The target is 11 μm thick and tilted at 1.3° to the probe. The gap separation is 100 μm. ICCD camera is gated at 20 ns.

An X-ray streak camera (Hamamatsu Photonics

C4575-03) captured the emissions related to the implosion and heating of the double foils. From the 50-μm slit, we estimated the spatial resolution to be 54 μm. The observation is normal to the laser axis and tilted at 1.3° to the target surface. The image is magnified 7.0 times. We used a full-window range of 1.1 ns. The 30-nm Au-coated 100-nm-parylene-N cathode detects photons in the region from 20 eV to 5 keV.

FIGURE 3(a) shows a streak image of the imploding foils. The implosion beams (long beams) peak at 0 ns and the heating beams (short beams) are delayed by 0.3 ns. Core emission is not observed, although the core plasma must be formed around 1.3 ns. FIGURE 3(b) shows the image for the heating beam of a 1.1-ns delay. No clear core emission is shown, except for some shots showing weak core emissions. At a 1.3-ns delay, as shown in FIG. 3(c), the heating beams give three bright areas around the center, which are the central core spot (central circle), and the right and left ablation areas (side circles, ablation). FIGURE 3(c) is the same shot as that in FIG. 2. The 1.3-ns delay agrees with the maximum compression time, predicted by STAR 1D and FIG. 3(d) is another shot under the same condition as (c). The central emission is delayed by 50 ps from the side emissions and is much strong at (c). STAR 1D suggests that the side (Ablation) emissions are between the cutoff and the ablation surfaces and the central emission is at the imploded core. Although it seems that the side emissions close to the ablation surface are peeled off as time passes, the core stagnates again and emits X-rays for 300 ps full-width half maximum (FWHM) or more. These features are observed only when the heating beams are between 1.1 and 2.0 ns. If no heating beams are illuminated around this time, we observed neither core emissions, nor peripheral emissions.

The core emissions in FIGs. 3(c) and (d) are integrated in time and space over the central core area, and are plotted on the R-T diagram as shown by Diamonds in FIG. 4 against delay of the heating beams. If the heating beam timing is earlier than 1.1 ns, we do not observe any core emission, as shown in FIGs. 3(a) and (b). The first emission peak occurs at 1.3 ns, the timing of the core plasma collision. FWHM is 300 ps. This peak is followed by the weak peak after 600 ps. Both the target and laser parameters for each shot deviate, leading to a timing deviation of ±100 ps between the experiment and the simulation, as shown by the horizontal error. The vertical error bar is the shot-to-shot deviation (standard error) for every 10 shots.

FIGUREs 3 and 4 suggest that the imploded cold core is heated by the heating beam to emit X-ray radiations.

Three neutron detectors ND1, ND2 and ND3 are distributed around the chamber[11]. ND1 is at 1.28 m on the beam 1 axis, and ND2 at 1.25 m on the beam 2 axis, consisting both of a 10-cm-diam. and 10-cm-long plastic scintillator (BC408) coupled to a 1-inch-diameter photo-

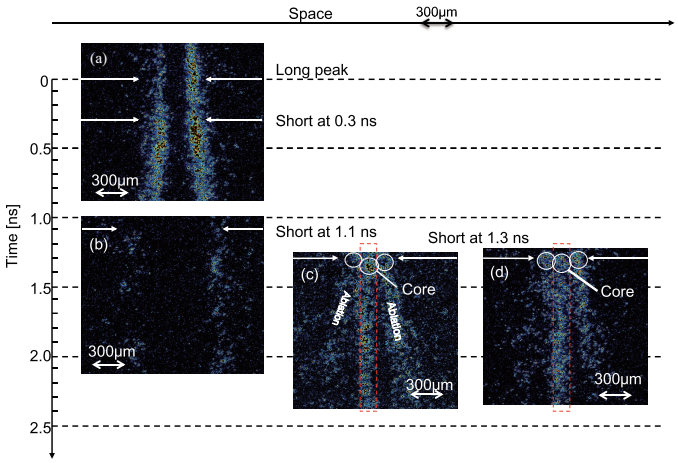

FIG. 3. X-ray streak image of the imploding-heating foils (a) at 0.3 ns delay. No core is formed. (b) At 1.1-ns delay, no core emission is seen. (c) and (d) At 1.3-ns delay, the core is heated. Three bright emissions are at the central core (circled) and at the peripheral (side) areas (circled). Ablation is the ablated plasma. The Au cathode detects emissions not less than 20 eV.

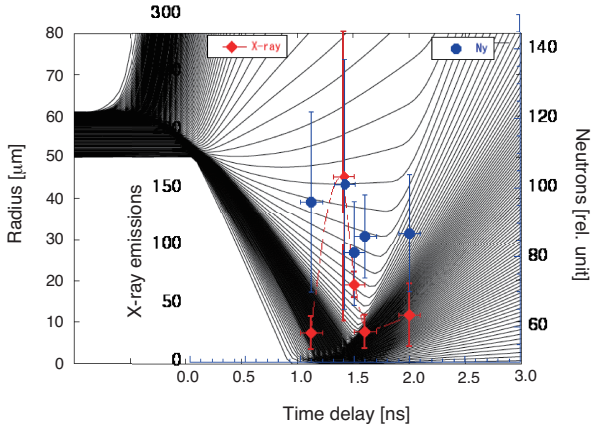

FIG. 4. Diamond : X-ray core-emissions versus the heating beam delay on R-T diagram. The vertical error bar is the shot-to-shot deviation (standard error) for every 10 shots. Dot : DD thermal neutron time of flight signal from ND3. The error bar is 1σ.

multiplier. ND3 is a 6-inch plastic scintillator (NE102, 15 cm in diameter and 6 cm in length) coupled to a 2-inch photomultiplier located 1.43 m from the target normal to the laser axis. The front side, as well as the other sides, is shielded by a 5-cm-thick lead plate, which reduces the number of the 2.45-MeV neutrons to 0.9 ×the incidence. The output is connected to a 5-GHz digital oscilloscope. The total temporal resolution is 4 ns. The detector was calibrated using a ^{252}Cf source (Eckert & Ziegler, A3036-2). ND3 captured 0 $\sim$ 2 neutrons per shot. After accumulating each 10 shots, we have filtered the low frequency noises less than 150 MHz out through a

Fast Fourier Transform filter, which reveals a small peak with a wide deviation around 1.4 ns as Dots in FIG. 4. The peak ($\sim 25\pm7$ mV) corresponds to a 1000 ± 280 yield for 4π angle. Neither ND1 nor ND2 has detected distinguishable neutron signals, maybe due to smaller scintillator and PMT volumes.

Since the simulation suggests the core density is compressed to 2×the solid CD density of 1.1 g/cm^3 at least, then the deuteron density will be $n_D = 9\times10^{22}$ cm^{-3}. Assuming the Z number of Carbon is ~ 4, the plasma density in the core will be $n_p = 6\times10^{23}$ cm^{-3}. If 30 % of the heating beams energy is absorbed into the plasma and is transported into the core of 30 μm diameter, and supposed the all particles in the core have the same temperature, then it will be 300 eV. This temperature can yield the neutrons N_y in τ of 300 ps stagnation period as $N_y = n_D^2/4 < \sigma v_{th} > V\tau \sim 2000$, where $< \sigma v_{th} >= 3.5\times10^{-25}$ cm^3/s and V is the core volume.

Using the electron density profile at the maximum compression calculated by STAR 1D, a 1D PIC (PICLS1d) studied the fast electron transport and energy deposition in the imploded plasmas. The preimploded plasmas are initially consisting of carbon and deuteron ions. The carbon (deuteron) ions are ionized at $Z = 2(1)$. They are ionized to a higher charge state through heating. The heating beam with a duration of 100 fs and a peak intensity of 2×10^{17} W/cm^2 is incident from the left boundary, which is an absorbing boundary for particles and electromagnetic waves. The right boundary is the mirror boundary used to simulate the heating beams at the right side of the imploded plasmas. The absorption of the laser energy is 33.8 %, which was small due to the 1D restriction. So that this PIC simulation underestimated the heating performance. FIGUREs 5(a) and (b) show the electron and the deuteron phase plots and temperature distributions observed at 600 fs and 4 ps, respectively. Two groups of hot electrons with 50 and 200 keV in quasi-Maxwellian distributions are produced by the short pulse. The lower energy group contains ponderomotive electrons, which carry most of the absorbed energy. These electrons slow down and deposit energy below $X \sim 50\,\mu$m via collisions. Higher energy electrons are produced below the critical density via plasma waves excitation. These energetic electrons are transported through the imploded plasma and are scattered by the ions.

Because the lower hot electrons deposit energy and heat the bulk electrons owing to the short stopping range, the electron bulk temperature below $\sim 20n_c$ is greater than 100 eV. The core region is also heated up diffusively to ~40 eV electron temperature at 4 ps. At this time the plasma is not thermally equilibrated, and the ion temperature is slightly over 20 eV. The bulk electron energy is transferred to ions over tens picoseconds. So we expect the core temperature would be $\sim$ 30 eV, which is higher than 20 eV, the detectable temperature of the streak camera, as we see in FIGs. 3 (c) and (d).

The optimum location where ions are most effectively heated is obtained by the relaxation rate determined by the local temperature and density. At these conditions, deuterons are heated effectively around $X \sim 50\,\mu$m, as shown in FIG. 5(b). This location could be shifted to the higher density by increasing the hot electron temperature or the energy of the heating pulse. The deuterons' mean energy is a few hundred eV, which is the appropriate temperature for initiating the fusion reaction. The energy is used for producing measurable thermal neutrons. The optimization of the heating laser to achieve the efficient core heating is planned in the further study.

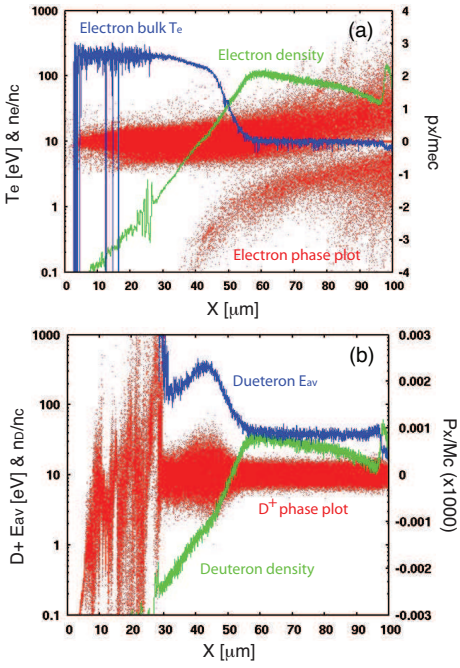

FIG. 5. 1D PIC: (a) Electron phase plot of axial momentum p_x, electron density n_e/n_c(green), and bulk temperature $\log T_e$(blue) observed at 600 fs. (b) D^+ phase plot of axial momentum P_x. and deuteron average energy (blue) observed at 4 ps. Laser is incident from the left side to the cutoff at X = 20 μm, where the strong plasma waves are excited. Position X = 100 μm is the core center.

We have proposed a compact fast heating experiment to initiate a fusion reaction and to clarify its dynamics. Using a simple implosion scheme, we showed that the hot electrons deposit energy to the peripheral plasma before reaching the ablation surface and also they reach the core and deposit some energy in it to emit X-ray radiations. Based on the neutron yields observed in the experiment the core is supposedly heated up to a few hundred electronvolts as long as the core stagnates. The results are promising for promoting the laser fusion. This core temperature based on the neutron yields is higher than the calculation by the 1D hydrodynamic-PIC simulation probably due to the lower absorption of the heating

pulse. The proposed compact experiment is an interesting testbed of the fast ignition.

GPI was supported in part by KAKENHI (21244088), the Science Research Promotion Fund of the Promotion and Mutual Aid Corporation for Private Schools of Japan, and NIRS. Y. S. was sponsored in part by DOE grant No. DE-PS02-08ER08-16.

* kitagawa@gpi.ac.jp

[1] M. Tabak *et al.*, Phys. Plasmas **1**, 1626 (1994).
[2] Y. Kitagawa *et al.*, IEEE J. Quantum Electron. **71**, 281-293 (2005).
[3] R. Kodama *et al.*, Nature(London) **412**, 798-802 (2001).
[4] R. Kodama *et al.*, Nature(London) **418**, 933-934 (2002).
[5] Y. Kitagawa *et al.*, Phys. Rev. E **71**, 016403 (2005).
[6] S. Atzeni and J. Meyer-ter-vehn, *the Physics of Inertial Fusion*, ch.12, Qxford Scienece Public. (Clarendon Press-Oxord, 2004).
[7] Y. Sentoku *et al.*, Phys. Plasmas **11**, 3083 (2004).
[8] R. Jung *et al.*, Phys. Rev. Lett. **94**, 195001-1-4(2005).
[9] A. L. Lei *et al.*, Phys. Rev. Lett. **96**, 255006 (2006).
[10] N. Naumova *et al.*, Phys. Rev. Lett. **102**, 025002 (2009).
[11] Y. Kitagawa *et al.*, Plasma Fusion Res. **6**, 1306006 (2011).
[12] T. Kurita *et al.*, Trans.IEE Japan. C, Electronics, Inf. and Sys. Soc. **128(5)**, 707-712 (2008).
[13] H. Yoshida et al., Optics Lett. **28**, 257-259(2003).
[14] R. Yasuhara *et al.*, Opt. Lett. **33**, 1711 (2008).
[15] A. Sunahara *et al.*, Plasma Fusion Res. **3**, 043-1-5 (2008).